NIH Public Access
Author Manuscript
Biomaterials. Author manuscript; available in PMC 2011 July 01.

Published in final edited form as:
Biomaterials. 2010 July ; 31(21): 5598–5607. doi:10.1016/j.biomaterials.2010.03.010.

Translocation of Cell Penetrating Peptide Engrafted Nanoparticles Across Skin Layers

Ram R Patlolla[1], **Pinaki Desai**[1], **Kalayu Belay**[2], and **Mandip Singh**[1,*]

[1]College of Pharmacy and Pharmaceutical Sciences. Florida A&M University, Tallahassee, FL 32307, USA, Tel: 850-561-2790; Fax: 850-599-3813.

[2]Department of Physics, Florida A&M University, Tallahassee.

Abstract

The objective of the current study was to evaluate the ability of cell penetrating peptides (CPP) to translocate the lipid payload into the skin layers. Fluorescent dye (DID-oil) encapsulated nano lipid crystal nanoparticles (FNLCN) were prepared using Compritol, Miglyol and DOGS-NTA-Ni lipids by hot melt homogenization technique. The FNLCN surface was coated with TAT peptide (FNLCNT) or control YKA peptide (FNLCNY) and in vitro rat skin permeation studies were performed using Franz diffusion cells. Observation of lateral skin sections obtained using cryotome with a confocal microscope demonstrated that skin permeation of FNLCNT was time dependent and after 24 h, fluorescence was observed upto a depth of 120 μm which was localized in the hair follicles and epidermis. In case of FNLCN and FNLCNY formulations fluorescence was mainly observed in the hair follicles. This observation was further supported by confocal Raman spectroscopy where higher fluorescence signal intensity was observed at 80 and 120 μm depth with FNLCNT treated skin and intensity of fluorescence peaks was in the ratio of 2:1:1 and 5:3:1 for FNLCNT, FNLCN, and FNLCNY treated skin sections, respectively. Furthermore, replacement of DID-oil with celecoxib (Cxb), a model lipophilic drug showed similar results and after 24 h, the CXBNT formulation increased the Cxb concentration in SC by 3 and 6 fold and in epidermis by 2 and 3 fold as compared to CXBN and CXBNY formulations respectively. Our results strongly suggest that CPP can translocate nanoparticles with their payloads into deeper skin layers.

Keywords

Nanoparticles; TAT peptide; Topical delivery; Transdermal delivery; Cell Penetrating Peptides

1. Introduction

Topical drug delivery offers several advantages over the conventional oral and intravenous dosage forms such as prevention of first pass metabolism, minimization of pain and possible controlled release of drugs. There is a growing interest in the optimization of drug delivery targeting to the physiological site in the skin [1,2]. Several attempts have been made and are still under investigation to develop a topical formulation for micro and macromolecules for the treatment of skin diseases. The success of topical delivery depends on the ability of drug

*To whom correspondence should be addressed (mandip.sachdeva@gmail.com).

Publisher's Disclaimer: This is a PDF file of an unedited manuscript that has been accepted for publication. As a service to our customers we are providing this early version of the manuscript. The manuscript will undergo copyediting, typesetting, and review of the resulting proof before it is published in its final citable form. Please note that during the production process errors may be discovered which could affect the content, and all legal disclaimers that apply to the journal pertain.

NIH-PA Author Manuscript
NIH-PA Author Manuscript
NIH-PA Author Manuscript

NIH-PA Author Manuscript

NIH-PA Author Manuscript

NIH-PA Author Manuscript

to permeate the skin in sufficient quantities to achieve its desired therapeutic effects. Most drug candidates alone are unable to cross the stratum corneum and require physical enhancers or special transporters to enter into the skin [3]. Chemical enhancers are widely used for the topical delivery of active agents that modulate the penetration of macromolecules across the skin but have limited success [4, 5]. Previous studies in our laboratory [6, 7] and others [8] have shown that the permeation of melatonin across the skin can be increased significantly using chemical penetration enhancers in solution formulations. Chemical penetration enhancers such as fatty alcohols and fatty acids increased the permeation of melatonin across the skin and the enhancement of permeation was found to be dependent on the chemical structure of the enhancers [6]. Apart from chemical enhancers, other techniques used to enhance the skin permeation of active ingredients are electroportation, iontophoresis and microneedles [9]. However, each of these techniques has their respective problems in terms of toxicity and therapeutic feasibility. An alternative delivery strategy is the use of nanoparticle delivery systems which are known to be biocompatible and protect the active ingredient from degradation. Among several nanoparticle systems, lipid nanoparticles are promising as drug carrier system for skin application. Melt-emulsified nanoparticles, such as solid lipid nanoparticles, have several advantages over nanoemulsions, nanosuspensions, mixed micelles, polymeric nanoparticles and liposomes [10, 11]. Solid lipid nanoparticles protect the active ingredients from enzymatic degradation, prevent transepidermal water loss and release the drugs in controlled manner for prolonged period and thereby enhance the therapeutic effect [12]. It has been shown that stabilization of chemically unstable drugs by incorporating into a lipid matrix [12] and also sustained release is possible due to solid matrix properties of solid lipid nanoparticles [13]. Solid lipid nanoparticles are composed of physiological lipids with low toxicity profile and can find application not only in cosmetic and dermatological preparations but also in parenteral and oral drug formulations [14, 15]. Many drugs have been successfully incorporated into solid lipid nanoparticles but their use is restricted due to: a) low drug loading, and b) drug expulsion from the carrier which leads to a decrease of the chemical stability of drug molecules during storage. Therefore, to decrease the degree of organization and increase the drug loading, nano lipid crystal (NLC) nanoparticles have been developed and reported as the second generation of lipid nanoparticles [16]. Based on the chemical nature of the lipid molecules, the inner structure of NLC is different from that of SLN because the former is composed of mixtures of solid and liquid lipids (oils). The solubility of active ingredients in oils is generally much higher than in solid lipids. For that reason, the higher drug loading capacity and minimal expulsion during storage could be achieved by the development of NLC [15]. The NLC possess similar characteristics as that of SLN and also has occlusive properties due to film formation on the skin surface. Several studies with NLC particles demonstrated that these particles do not cross the stratum corneum barrier and due to the occlusive property, the particles reside in the stratum corneum and release the drug into the epidermis. The strategies that enhance the skin permeation of NLC are worth investigating and useful for the treatment of various skin disorders, where the target site is in the deep epidermis.

Cell penetrating peptides (CPP) are emerging as attractive drug delivery tools because of their ability to translocate micro and macromolecules across the cell membrane [17]. CPP have been used to deliver several proteins [18], oligonucleotides [19], solid lipid nanoparticles [20] and liposomes [21] into tumor cells. There are only very few studies which have demonstrated that the skin permeation of cyclosporine and P20 peptides are enhanced when conjugated to the CPP [22]. The CPPs are mainly composed of arginine and lysine residues which confer positive charge to the CPP and several CPPs currently available have membrane translocating capability based on their arginine content. Among several CPPs, transactivating transcriptional activator (TAT) peptide is widely studied and extensively used for drug delivery. Lopes et al. showed that TAT and YARA cell

NIH-PA Author Manuscript

NIH-PA Author Manuscript

NIH-PA Author Manuscript

penetrating peptides are able to translocate P20 peptide across the human skin [22]. The objective of the current study was to understand the skin permeation of CPP coated nanoparticles into the skin. In the present study NLC formulated with DOGS-NTA-Ni spacer (NLCN) will be used for the encapsulation of anti-inflammatory molecule with surface modification by TAT peptide.

2. Materials and Methods

2.1. Materials

Celecoxib (Cxb) was a generous gift from Pfizer (Skokie, IL). The triglyceride Miglyol 812 and Compritol 888 ATO were kind gift samples from Sasol Germany GmbH (Witten, Germany) and Gattefosse (Saint Priest, France). 1,2-dioleoyl-*sn*-glycero-3-[(*N*-(5-amino-1-carboxypentyl) imidodiacetic acid) succinyl nickel salt] (DOGS-NTA-Ni) was purchased from Avanti Polar lipids (USA). Tetrahydrofuran, tween 80 and dialysis membrane (flat width of 23 mm) were procured from Sigma-Aldrich Chemicals (St. Louis, USA). Polyoxyethylene-20 oleyl ether (Volpo-20) was a kind gift from Croda Inc (New Jersey, USA). Vivaspin centrifuge filters (Molecular weight Cut off: 10, 000 Daltons) were procured from Sartorius Ltd, (Stonehouse, UK). Fetal bovine serum (FBS), antibiotics and lipophilic fluorescent dyes, Dio dye (excitation 484 nm and emission 501 nm) and DID-oil (excitation 644 nm and emission 665 nm) were procured from Invitrogen Corp (Eugene, OR). The H460 human NSCLC cell line was obtained from American Type Culture Collection (Rockville, MD, USA). H460 cells were grown in RPMI medium (Sigma, St. Louis, MO, USA) supplemented with 10% FBS. All tissue culture media contained penicillin (5000 U/ml), streptomycin (0.1 mg/ml), and neomycin (0.2 mg/ml). The cells were maintained at 37°C in the presence of 5% CO_2 in air. All other chemicals used in this research were of analytical grade. The six histidine tagged TAT (YGRKKRRQRRR-6 histidine tag, MW: 1560) cell penetrating peptide and control YKA (YKALRISRKLAK-6 histidine tag, MW: 1447) peptide were synthesized by GenScript Corporation (NJ, USA).

2.2. Animals

CD®(SD) hrBi hairless rats (250–300 g; Charles River Laboratories, Wilmington, MA) were utilized for the studies. The in-vitro skin permeation experimental protocol was approved by the Animal Care and Use Committee, Florida A & M University. The animals were acclimatized to laboratory conditions for one week prior to experiments and were on standard animal chow and water *ad libitum*. The temperature of the room was maintained at 22 ± 1 °C and the relative humidity of the experimentation room was in the range of 35–50 %.

2.3. Nanoparticle Preparation

The fluorescent dye encapsulated NLCN (FNLCN) formulation was prepared by hot melt homogenization technique [13]. In brief, 0.001 % w/w of DID-oil was dissolved in chloroform and mixed with lipid phase comprised of Compritol (7.0 % w/w), DOGS-NTA-Ni (0.02% w/w) and Miglyol (3.0 % w/w). “Later, organic phase was removed from the lipid phase on a rotary evaporator for 2–3 h at 80 °C and aqueous solution (20 ml) containing tween 80 (2.4 % w/w) was added to the lipid phase at the same temperature under high speed mixing (20,000 rpm for 1 min)”. The resultant oil-in-water dispersion was passed through Nanodebee® (Ottawa, Canada), high-pressure homogenizer at 20,000 psi for 5–6 cycles. Control FNLC formulation was prepared without DOGS-NTA-Ni similar to FNLCN except instead of DID-oil, Dio fluorescent dye was used. Further Cxb, a lipophilic non-steroidal anti-inflammatory drug encapsulated NLCN (CXBN) was prepared by dissolving the Cxb in dichloromethane and processed similar to FNLCN.

NIH-PA Author Manuscript

NIH-PA Author Manuscript

NIH-PA Author Manuscript

2.4. Characterization of nanoparticles

The particle size and zeta potential of NLCN formulations were measured using Nicomp 380 ZLS (Agilent Technologies, USA). The Nicomp 380 ZLS analyzer uses dynamic light scattering to obtain the essential features of the particle size distribution. In order to verify the total amount of Cxb present in the system, 0.1 ml of CXBN formulation was dissolved in 0.9 ml of tetrahydrofuran and subsequent dilutions were made with acetonitrile. For HPLC analysis for Cxb content, samples were centrifuged at 13,000 rpm for 15 min and 100μl of supernatant was injected into the HPLC. Entrapment efficiency was determined as reported earlier using vivaspin columns [23]. Vivaspin centrifuge filters consist of a filter membrane (molecular weight cut-off 6000–8000 Daltons) at the base of the sample recovery chamber. The CXBN (0.5 ml) formulation was placed on top of the vivaspin centrifuge filter membrane and centrifuged at 3500 rpm for 15 min. The amount of Cxb present in the aqueous phase was estimated using high-performance liquid chromatography (HPLC).

2.5. Binding Assay

Binding assay was carried out to determine the peptide (six histidine-TAT peptide) to DOGS-NTA-Ni ratio as per reported method [24]. In brief, for the binding assay, adherent H460 cells were seeded at a density of 1×10^5 cells/well in a 24-well plate. When cells were more than 80% confluent, the medium was replaced with fresh 0.5 ml of RPMI medium (supplemented with 10% Fetal Calf Serum and antibiotics). Before incubation of FNLCN (50 μl) with H460 cells, FNLCN (50 μl) were incubated with various amounts (6.4, 12.8 and 25.6 μg) of six histidine-TAT peptide for 30 minutes at RT to generate FNLCNT. Cells were incubated with nanoparticle formulations for 1 h at 4°C. After the incubation, cells were washed three times with cold phosphate buffer saline (PBS, pH7.4) and suspended in 2% paraformaldehyde. Cell associated fluorescence was determined using flow cytometry.

2.6. Visualization of FNLCN by Confocal Laser Scanning Microscopy

Hairless rats (CD® (SD)HrBi, Male) were sacrificed by an overdose of halothane anesthesia. The skin from the dorsal surface was excised and the adherent fat and subcutaneous tissue was removed. The skin was mounted between the donor and receptor compartments of the Franz diffusion cells (Permegear Inc., Riegelsville, PA) with the stratum corneum facing the donor compartment. Each cell had a diffusional surface area of 0.636 cm^2. The FNLCNT and FNLCNY formulations were prepared by incubating the FNLCN formulation with the TAT and YKA peptide at 1:1 weight ratio of DOGS-NTA to peptide. The formulation was applied to the epidermal side in the donor compartment and the receptor compartment was filled with pH 7.4 PBS with 10% w/v ethanol. The temperature of the receptor compartment was maintained at 37 ± 0.1°C with an external, constant temperature circulator water bath. The skin permeation studies were performed under un-occlusive conditions where water evaporation was allowed. In all subsequent skin permeation studies similar conditions were used. At predetermined time intervals (6, 12 or 24 h) the skin was taken out from the diffusion cell and blotted dry with Kimwipes® and the entire dosing area (0.636 cm^2) was punched out with a biopsy punch. For visualization of skin associated fluorescence, at the end of the study skin was collected and thin sections of 20–30 μm thick vertical sections were collected using a cryotome as reported earlier [25]. In case of lateral skin sections, first two sections with a thickness of 20 μm and remaining three sections of 40 μm were collected to represent the total skin depth of 160 μm. The skin sections were visualized with a confocal microscope (Leica, USA) using 10× objective and throughout the study period the instrument settings were constant for FNLCN, FNLCNT and FNLCNY treated samples.

NIH-PA Author Manuscript

NIH-PA Author Manuscript

NIH-PA Author Manuscript

2.7. Raman Spectroscopy

The lateral skin sections were observed with HR800 Raman spectroscopy (Horiba Jobin Yvon, NJ) for fluorescence intensity by positioning the skin sections on microscope stage. The HR800 is an integrated confocal Raman system, where microscope is coupled confocally to an 800 mm focal length spectrograph equipped with two switchable gratings. The confocal Raman spectroscopy uses an internal HeNe laser of excitation of 632.8nm and maximum power of 17.0 mw. We used the 10× (numerical aperture of 0.25, working distance of 0.7 mm and spot diameter of 3.1 nm) objective and 200 μm confocal pin hole to acquire the fluorescence data. Throughout the study, all instrument settings were kept constant and exposure time never exceeded 20 sec. Instrument was calibrated and corrected for the instrument using a standard silicon wafer centered at 520.5cm^{-1}.

In the beginning test runs were made with FNLCN formulation to acquire Raman spectra over an extended range from 200–4000 cm^{-1} to determine the DID fluorescent dye prominent peaks. As a control, the Raman spectra of untreated rat skin sections were collected as a function of depth upto 120 μm below the surface of the skin sample. The rat skin alone and NLCN was used as control. During each experiment, the spectrum was optimized in real time before data was acquired over an extended range. Raman spectra of FNLCN formulations with and without TAT and YKA peptide for 24 h skin permeation samples were acquired over a 200–1600cm^{-1}range.

2.8. In-vitro CXBN release studies

In vitro drug release studies were conducted with a cellulose membrane (6000–8000 molecular weight cut off) using a USP apparatus 1 (basket) dissolution apparatus (Vankel, NC) for 72 h with the help of 900 ml of 0.1 % w/v volpo-20 in phosphate buffer saline (PBS) pH 7.4 as dissolution medium. Cellulose membranes were soaked overnight in dissolution medium. To the pre-swollen cellulose membrane bags 2 ml of CXBN formulation was placed and both the ends of bags were tied to prevent any leakage. Later, dialysis bags were carefully placed in the baskets and the baskets were rotated at 50 rpm for 72 h at 37.0 ± 0.1 °C. At regular time intervals, 1 ml of sample was collected and replaced with equal volume of dissolution medium. Amount of Cxb released into the medium was determined with the help of HPLC analysis. The experiments were carried out in triplicate.

2.9. Skin permeation of CXBN formulations

In case of CXBN skin permeation studies, 0.1 ml (0.075 mg of Cxb) of CXBN formulations were applied onto the epidermis and receptor compartment was filled with 0.1% w/v valpo in PBS (pH 7.4). The TAT (CXBNT) and YKA (CXBNY) peptide coated CXBN formulations were prepared similar to FNLCN formulations. For comparison, 1 mg/ml Cxb solution (Cxb-S) was prepared by dissolving known amount of Cxb in 10 %v/v ethanol and 2.4 %w/v tween 80 in polyethylene glycol (PEG 400). After 24 h of skin permeation, the fluid in the receptor compartment and skin dosing area was collected as mentioned earlier. After completion of the study, the stratum corneum was removed by tape stripping with Transpore™ tape and 10 strips were collected [25]. The underlying tissue was frozen at − 30 °C on a cryobar stage and sectioned with a Cryotome (Thermo-Shandon, 620 Electronic, Pittsburgh, PA, USA).

2.10. Cxb extraction from skin

The exposed skin was collected, homogenized with 0.5 ml of 1 M acetic acid using a tissue homogenizer. The tissue homogenate was boiled for 10 minutes and after cooling to room temperature 0.5 ml of acetonitrile was added. The vials were sonicated in a bath sonicator for 30 sec before vortexing for 1 min and finally all the tissue samples were centrifuged at

NIH-PA Author Manuscript

NIH-PA Author Manuscript

NIH-PA Author Manuscript

13,200 rpm for 15 minutes. The supernatant was collected and the extracts were analyzed for Cxb content using HPLC. A recovery experiment was conducted to validate the method of extraction of Cxb in the skin tissue. The experiments were performed in triplicate.

2.11. Cxb HPLC method

The HPLC analysis of Cxb was performed with minor modifications from a reported method [26]. Briefly, HPLC system was comprised of an auto sampler (model 717 plus), binary pump (model 1525), Waters UV photodiode array detector (model 996). The mobile phase consisting of acetonitrile, water, acetic acid (54:45:1% v/v) was pumped through the Symmetry C18 column (5 μm, 4.6 × 250 mm) at a flow rate of 1.0 ml/min and the eluent was monitored at 254 nm. The Cxb stock solution was prepared with acetonitrile and the serial working standard solutions were prepared in mobile phase. All injections were performed at room temperature.

2.12. Statistical analysis

The Cxb content of the skin tissue was expressed as μg per g of the tissue. Differences between the skin permeation of with and without CPP coated formulation and control Cxb formulations were examined using ANOVA and Tukey multiple comparison test. Mean differences with $P < 0.05$ were considered to be significant.

3. Results

3.1. Nanoparticle Characterization

In the present study we have prepared the NLCN formulation using triglycerides with a mean particle size of 180 ± 30 nm and polydispersity indices of 0.18. The zeta potential of FNLCN and CXBN formulations in double distilled water (pH 6.4) was − 15.24 and − 17.25 mV, respectively. The assay results indicated that approximately 0.75 mg/ml of Cxb was present in the formulation and the entrapment efficiency of CXBN was 85–90 %. The observed higher Cxb entrapment might be due to the liquid state of Miglyol oil, which helps to encapsulate the higher amount of lipophilic drugs and reduces the particle crystallinity which imparts better stability and higher suitability for controlled release [15].

3.2. Binding Assay

Fig. 1 shows the binding affinity of FNLCN formulation to H460 cells in presence of various amounts of TAT peptide. As the concentration of TAT peptide increased to 12.8 μg, the shift in fluorescence intensity was more than 100 folds (Fig. 1A) and further increase in TAT peptide concentration did not yield any further increase in fluorescence intensity. However, incubation of H460 cells with FNLCN formulations prepared without DOGS-NTA-Ni spacer did not show any fluorescence shift even in the presence of TAT peptide (Fig. 1B). In all subsequent studies, equal weight ratio (1:1 w/w) of DOGS-NTA to TAT or YKA peptide was used.

3.3. Tracking of fluorescent nanoparticles in the skin

Our preliminary studies with FNLC formulations found that, after 24 h nanoparticles were able to enter into the skin mainly through hair follicles and most of the dye was concentrated on the stratum corneum (Fig. 1S). Fig. 2 shows the skin permeation of FNLCN formulations tracked after 6, 12 and 24 h using a confocal microscope (10× objectives). At 6 h, the skin permeation of FNLCN was very minimal even in presence of TAT peptide and as the time progressed after 12 h more amount of skin associated fluorescence was observed in the stratum corneum and to some extent in the epidermis with FNLCNT. However, with FNLCN and NLCNY formulations, most of the fluorescence was observed in the

NIH-PA Author Manuscript

NIH-PA Author Manuscript

NIH-PA Author Manuscript

appendages after 24 h. It was observed that after 6 and 12 h more amount of the fluorescent dye was present in 20 μm skin sections, irrespective of TAT coating (Fig. 3 and 4). However, after 24 h, the TAT coated nanoparticles were observed in the deeper skin layers and the fluorescence were visible in the epidermal cells apart from appendages (Fig. 5).

3.4. Raman Spectroscopy

Fig. 2S shows that the intensity of fluorescence peaks were observed at 996, 946 and 776 cm^{-1} for the stratum corneum alone, NLCN and FNLCN formulations, respectively. In most cases the fluorescence spectra of biological samples are complex and overlapping making signal discrimination very difficult. However, in our study the fluorescence peaks were distinctly located and there was no overlap of fluorescent DID-oil dye peak with the blank NLCN and rat skin peaks (Fig. 2S). This was an important characteristic to study the degree of the permeation of the particles through the skin. Fig. 6 shows the fluorescence associated with the lateral skin sections following skin permeation for a period of 24h with FNLCN obtained using confocal Raman spectroscopy. At 80 μm depth, the intensities of fluorescence were 84.21 ± 10.31, 42.17 ± 6.4, and 36.24 ± 4.32 counts with FNLCNT, FNLCN and FNLCNY treated formulations, respectively. Whereas at 120 μm depth the intensities were reduced to 61.42 ± 9.24, 31.39 ± 711 and 11.50 ± 3.09 counts with FNLCNT, FNLCN, and FNLCNY treated formulations, respectively.

3.5. In-vitro Cxb release studies

The CXBN formulation was able to release the Cxb in controlled manner and complete drug (> 80 %) was released after 72 h (Fig. 7). The controlled release of Cxb from CXBN may be due to the long diffusion path length, i.e. Cxb has initiate the diffusion from Miglyol oil phase to the solid outer surface of the nanoparticles before undergoing partitioning between outer lipid and the bulk aqueous phase. Similar observations were made by Zhang *et al* [27] where solid lipid microparticles prepared with Compritol showed slower clozapine release comparing with microparticles made with tristearin mainly because of the distribution of clozapine in the inner area of the lipid matrix and longer diffusion path length.

3.6. In-vitro skin permeation of CXBN

The CXBN skin permeation experiment was carried out to correlate the observations made in the fluorescent visualization results and also to understand whether TAT peptide would translocate the drug pay load in significant amounts into various skin layers. Fig. 8 shows the effect of TAT peptide on the CXBN skin permeation at the end of 24 h period with full thickness rat skin. The CXBNT formulation showed 3 fold increases in stratum corneum Cxb concentrations compared with CXBN alone. With Cxb-S, CXBN, CXBNT and CXBNY formulations, the epidermal Cxb concentration after 24 h period was 3.59 ± 0.1, 37.28 ± 3.0, 92.94 ± 9.1 and 57.53 ± 8.1 μg/g of skin respectively.

4. Discussion

Skin is the largest organ of the body but due to the presence of a strong protective barrier, stratum corneum, therapeutic molecules are mostly administered through oral or parenteral routes for the treatment of skin infections. Chemical permeation enhancers are widely used as penetration enhancers but are unable to protect the drug molecules from degradation and clearance from the skin. Nanoparticles are able to overcome these problems but irrespective of nanomaterial used, they do not cross but possibly permeate into stratum corneum and release the drug in a controlled manner into the upper epidermis. Further, upon application of nanoparticles on the skin, the uptake is confined to upper epidermal layers without complete penetration into deeper skin layers. Although, the thickness of the stratum corneum is only about 20 μm, the actual diffusional path of most molecules crossing the skin

NIH-PA Author Manuscript

NIH-PA Author Manuscript

NIH-PA Author Manuscript

is of the order of 400 μm [28] thus greatly reducing the rate of drug penetration. Our objective is to enhance the skin permeation of nanoparticles using TAT peptide which is known for translocating small and large molecules across the cell membranes and skin layers [21–23].

In the present investigation the nanoparticle surface was modified with TAT peptide using a DOGS-NTA-Ni spacer. This approach exploits the interaction between chelated divalent metal ions such as nickel and a short sequence of histidine residues (four to ten repeating units) added to the N or C-terminus of the protein, referred to as histidine-tags (His-tag). The nitrilotriacetic acid-nickel (NTA-Ni) is extensively used in the purification of proteins and peptides. The standard methods such as covalent and non-covalent attachment of proteins and peptides to the lipid surfaces are time consuming, difficult to work with small quantity of materials, expensive to produce and purification process following chemical conjugation is tedious. Our objective is to use a simple and efficient method to conjugate the peptide onto the NLC surface using metal chelating lipids as spacer to bind with His tag for surface modification [29]. In case of Ni^{2+}, which has six coordination sites, NTA forms a strong complex with four of the metal sites, leaving two additional sites for interaction with the His tag present on the protein. The presence of 4–10 contiguous histidine groups on either end (N or C terminal end) of the peptide are proven to be sufficient to bind the metal chelating lipids [29]. In the present study, we used six histidine groups at the N-terminal end of the peptides to conjugate on to the NLCN surfaces. The H460 cell binding assay results show that as the concentration of CPP increased from 0 to 12.8 μg, there was a 100 fold increase in fluorescence shift indicating that the spacer is on the surface of the nanoparticles which led to the increase of six histidine tagged TAT peptide binding affinity to the NLCN. Furthermore, addition of TAT peptide to the FNLC prepared without DOGS-NTA-Ni spacer did not show any significant increase in fluorescence shift thus suggesting that there is no non-specific interaction between nanoparticles and six histidine tagged TAT peptide.

To understand the translocation of TAT peptide coated nanoparticles into the skin, the in vitro skin permeation studies were carried out using fluorescent dye encapsulated nanoparticles. After completion of skin permeation study, the 30 μm thick vertical skin sections were collected using a cryotome and the skin associated fluorescence was observed with a confocal microscope. The skin permeation of TAT peptide coated nanoparticles was found to be time dependent; after 6 h the fluorescence was concentrated in the stratum corneum and after 12 h the fluorescent dye was seen in the epidermis of TAT peptide treated skin samples. In general due to rigid nature of NLCN, the particles are unable to cross the stratum corneum in intact form [30]. Furthermore, NLCN prepared with triglycerides such as Miglyol and Compritol will have negative charge on their surfaces and will have less affinity towards the cell surfaces and skin. This is also evident from zeta potential measurement of TAT peptide coated and uncoated NLCN formulations, where NLCN particles had a charge of − 15 mV and surface modification with TAT peptide reduced the zeta potential to − 4 mV. Jung et al [31] showed that negatively charged liposomes will have lowest skin penetration in contrast to cationic liposomes similar observations were also made by other workers [32]. Nanoparticles prepared with cationic polymer, chitosan have shown to enhance the skin permeation of siRNA and small molecules [33] mainly because of presence of positively charged amine groups on the chitosan surface which strongly binds to the skin and thereby enhances skin permeation. One of the reasons for increased skin permeation of TAT peptide coated nanoparticle formulation is the presence of positively charged arginine groups in TAT peptide sequences, which will have high binding affinity towards the cell surfaces and also towards the skin [23,34]. This is confirmed by our results which showed that modification of NLCN surface with TAT peptide enhanced the skin permeation and most of the fluorescence was observed in the epidermis and upper dermis

NIH-PA Author Manuscript

NIH-PA Author Manuscript

NIH-PA Author Manuscript

after 24 h (Fig. 5). In case of FNLCN and FNLCNY formulation treated skin, the fluorescence was mainly localized on the stratum corneum surface.

To further assess the effect of TAT peptide on skin permeation of nanoparticles, after 12 and 24 h of skin permeation, lateral skin sections were collected with varying thicknesses to represent stratum corneum and different depths of epidermis. After 12 h, the TAT peptide treated skin samples showed higher fluorescence in the epidermal cells which are closer to the hair follicles indicating a possibility for lateral infiltration of TAT peptide (unpublished observation). Furthermore, with FNLC, FNLCN and FNLCNY formulations, fluorescence was seen in the appendages (Fig. 2–5) indicating that these conventional formulations were unable to cross the stratum corneum and instead accumulate mainly in the upper layers of the skin. The depth profiling of FNLCN skin permeation showed that after 24 h, distinct fluorescence was seen upto a depth of 120 μm in the lateral skin sections treated with FNLCNT formulations, where as with the FNLCN formulation treated skin, the fluorescence was visible only in the appendages upto a depth of 120 μm. However, with FNLCNY formulation, the fluorescence was present in the appendages to a depth of 80 μm (Fig. 5). Irrespective of type of nanomaterial used, most of the nanoparticles (lipid or polymeric) will be able to enter into stratum corneum but unable to permeate into deeper portions of the epidermis [35, 36]. Studies conducted by Wu et al (28) clearly demonstrate that fluorescent polymeric nanoparticles could penetrate the deeper layers of stratum corneum and were also associated with hair follicles which is similar to our observations. This further gives credence to our studies where coating the nanoparticles with TAT (FNLCNT) enhanced their deposition to deeper layers of epidermis. The main pathway involved in the nanoparticles translocation into the skin is hair follicles but skin appendages occupy only a small fraction (1/1000) of the entire skin surface area and consequently, very little drug actually crosses the skin via the follicular route. Nanoparticles are unable to enter into the skin via transcellular pathway, which need specialized mechanism and very few drugs and CPP have the properties to enter the skin via this pathway. The TAT peptide initiated nanoparticle translocation involves the following sequence of events a) during early time points positively charged arginine groups in TAT peptide bind to the stratum corneum b) as time progresses, water evaporates from the formulation and forms a thin lipid layer on the skin surface c) occlusive property of nanoparticles facilitate their entry into the stratum corneum and from that point TAT peptide plays a major role in further movement of nanoparticles into the deeper epidermal layers. The permeation of TAT peptide coated nanoparticles was minimal (unpublished observation) when water evaporation from the formulation was prevented and this demonstrates the effect of occlusion on permeation of nanoparticles in the skin.

In the literature there is no convincing evidence about the CPP penetration into the cells and also translocation into the skin. Trehin et al [37] studied the TAT peptide permeation in Calu-3 cells (human bronchial submucosal adenocarcinoma cells) using confocal laser scanning microscopy and demonstrated that the TAT peptide uptake was mainly confined to extracellular space and most of the fluorescence staining was observed at the tight junctions.

To further support the confocal microscopy observations, we quantified the skin associated fluorescence using confocal Raman spectroscopy. In recent years, Raman spectroscopy has been used in combination with confocal imaging system which provides additional advantage such as real time analysis of nanoparticles permeation into the skin [38, 39]. Confocal Raman spectroscopy is an emerging nondestructive technique to study the morphology and interaction of biomaterials with the biological tissues under in vitro and in vivo conditions. Caspers et.al [40] used confocal Raman spectroscopy to depth profile and obtained the molecular composition of a human skin with high spatial resolution. Though confocal Raman spectroscopy is non destructive technique, in our studies, skin associated

NIH-PA Author Manuscript

NIH-PA Author Manuscript

NIH-PA Author Manuscript

fluorescence was analyzed using lateral skin sections obtained with cryotomy. We adopted this procedure to prevent the interference of surface bound fluorescent dye in depth profiling mainly because of the fact that the current procedure minimizes the extinction of the Raman signals that result due to scattered contributions originating from a diffraction-limited laser focal volume and the refractive index of the sample as the illuminated volume is slowly moved further into or defocused above the sample. Furthermore, to prevent photo bleaching, the exposure time was kept not more 20 sec. The 10× objective was selected because of its ability to collect data from a bigger volume of the sample (spatial diameter of 3.1 nm). In these studies, 20 and 40 μm lateral skin sections were discarded because the upper skin layers are irregular in shape and cannot differentiate the fluorescence intensity among the formulations. After 24 h of skin permeation, there was increase in fluorescence intensity with FNLCNT formulation compared to FNLCN and FNLCNY formulations at 80 and 120 μm depths. Observation of lateral skin sections under confocal Raman spectroscopy showed that at 80 and 120 μm depths, there was 2–3 fold increase in fluorescence intensity with TAT peptide modified FNLCN compared to FNLCN and control FNLCNY formulations (Fig. 6). These results are complimentary to the confocal microscope observations wherein after 24 h of skin permeation the continuous fluorescence was observed in TAT peptide treated skin samples at a depth of 120 μm.

For better understanding of skin permeation enhancement ability of TAT peptide, we prepared Cxb, a model NSAID, encapsulated NLCN formulations. The lipophilic Cox-2 inhibitor, Cxb, was successfully encapsulated in the NLC nanoparticles using Compritol and Miglyol. CXBN formulation was able to release the Cxb in controlled manner for prolonged period of time. The release studies demonstrated that, at initial 8 h, CXBN formulation released 8–10 % of Cxb and after 24 h the release was 34 % indicating that the Cxb was encapsulated in the NLCN. Surface modification of nanoparticles with TAT peptide increased the skin permeation of Cxb significantly into SC and epidermal layers compared to control CXBN and CXBNY formulations (Fig. 8). There are very few studies which have shown the skin permeation of SLN and NLC nanoparticles into epidermal layers where encapsulated nile red, a lipophilic fluorescent dye, was released into the deeper skin layers as observed with confocal microscope [41]. However, the literature strongly suggests that entry of intact nanoparticles alone into the epidermis is not possible and maybe traces of lipids or dye released from the nanoparticles might enter into the deeper skin layers [28, 35]. Furthermore, there is no experimental evidence so far which shows that CPP can translocate the lipid or polymer payload into the skin. Very few studies have shown an increase in skin permeation of peptides when conjugated to the CPPs [22, 32]. Our observations with CXBNT formulation suggest that after 24 h, the CXBNT formulation showed increase in Cxb concentration in stratum corneum by 3 and 6 fold and in epidermis by 2 and 3 fold as compared to CXBN and CXBNY formulations, respectively (Fig. 8). There is considerable evidence that arginine groups play pivotal role in the TAT peptide skin permeation enhancement activity, where replacement of TAT peptide with YKA peptide did not lead to any significant permeation because YKA peptide contains only one arginine group [22, 23]. This indicates that surface modification with TAT peptide enhanced the Cxb permeation through full thickness rat skin over a period of time. The control Cxb-S formulation prepared with 10% ethanol in PEG400 showed lower skin retention compared to nanoparticle formulations.

5. Conclusions

Our studies indicate that TAT peptide enhanced the skin permeation of nanoparticles by translocating the nanoparticles across the skin layers to a depth of 120 μm. Our results also suggest that CPP can be used to cargo the lipid pay loads into the skin and this strategy can also be applicable for the delivery of not only NLCN but also for liposomes and polymeric

NIH-PA Author Manuscript

NIH-PA Author Manuscript

NIH-PA Author Manuscript

nanoparticles. Our future studies aimed to understand the TAT peptide nanoparticles translocation under in vivo conditions.

Supplementary Material

Refer to Web version on PubMed Central for supplementary material.

Acknowledgments

We thank Ruth Didier, College of Medicine, Florida State University Tallahassee for her kind help in Confocal Microscopy studies. The authors acknowledge the financial assistance provided by NIAMS (NIH) grant number AR47455-02 and RCMI (NIH) grant number G12RR03020.

Abbreviations

NLC	Nano lipid crystal nanoparticles without DOGS-NTA-Ni
NLCN	DOGS-NTA-Ni containing Nano lipid crystal nanoparticles
FNLCN	fluorescent dye encapsulated NLCN
FNLCNT	TAT coated FNLCN
FNLCNY	YKA coated FNLCN
FNLC	fluorescent dye encapsulated NLC
Cxb	Celecoxib
CXBN	Cxb encapsulated NLCN
CXBNT	TAT coated CXBN
CXBNY	YKA coated CXBN
Cxb-S	Cxb solution
DOGS-NTA-Ni	1,2-dioleoyl-*sn*-glycero-3-[(*N*-(5-amino-1-carboxypentyl) imidodiacetic acid) succinyl nickel salt]
CPP	Cell Penetrating Peptide

References

1. Barry BW. Novel mechanisms and devices to enable successful transdermal drug delivery. Eur J Pharm Sci. 2001; 14:101–114. [PubMed: 11500256]
2. Williams, AC. Transdermal and Topical Drug Delivery: From Theory to Clinical Practice. London: Pharmaceutical Press; 2003.
3. Trommer H, Neubert RHH. Overcoming the stratum corneum: the modulation of skin penetration. Skin Pharmacol Physiol. 2006; 19:106–121. [PubMed: 16685150]
4. Prausnitz MR, Langer R. Transdermal drug delivery. Nat Biotechnol. 2008; 26:1261–1268. [PubMed: 18997767]
5. Sapra B, Jain S, Tiwary AK. Percutaneous permeation enhancement by terpenes: mechanistic view. AAPS J. 2008; 10(1):120–132. [PubMed: 18446512]
6. Kikwai L, Kanikkannan N, Babu RJ, Singh M. Effect of vehicles on the transdermal delivery of melatonin across porcine skin in vitro. J Control Release. 2002; 83(2):307–311. [PubMed: 12363456]
7. Andega S, Kanikkannan N, Singh M. Composition of the effect of fatty alcohols on the permeation of melatonin between porcine and human skin. J Control Release. 2001; 77(1–2):17–25. [PubMed: 11689256]

NIH-PA Author Manuscript

NIH-PA Author Manuscript

NIH-PA Author Manuscript

8. Dubey V, Mishra D, Asthana A, Jain NK. Transdermal delivery of a pineal hormone: melatonin via elastic liposomes. Biomaterials. 2006; 27(18):3491–3496. [PubMed: 16513163]
9. Kolli CS, Banga AK. Characterization of solid maltose microneedles and their use for transdermal delivery. Pharm Res. 2008; 25(1):104–113. [PubMed: 17597381]
10. Hou D, Xie C, Huang K, Zhu C. The production and characteristics of solid lipid nanoparticles (SLNs). Biomaterials. 2003; 24(10):1781–1785. [PubMed: 12593960]
11. Wang JJ, Liu KS, Sung KC, Tsai CY, Fang JY. Skin permeation of buprenorphine and its ester prodrugs from lipid nanoparticles: lipid emulsion, nanostructured lipid carriers and solid lipid nanoparticles. J Microencapsul. 2009; 13:1–14. [PubMed: 19225974]
12. Jenning V, Schafer-Korting M, Gohla SH. Vitamin A-loaded solid lipid nanoparticles for topical use: drug release properties. J Control Release. 2000; 66:115–126. [PubMed: 10742573]
13. Souto EB, Wissing SA, Barbosa CM, Muller RH. Development of a controlled release formulation based on SLN and NLC for topical clotrimazole delivery. Int J Pharm. 2004; 278:71–77. [PubMed: 15158950]
14. Almeida AJ, Souto E. Solid lipid nanoparticles as a drug delivery system for peptides and proteins. Adv Drug Deliv Rev. 2007; 59:478–490. [PubMed: 17543416]
15. Muller RH, Radke M, Wissing SA. Solid lipid nanoparticles (SLN) and nanostructured lipid carriers (NLC) in cosmetic and dematological preparations. Adv Drug Deliv Rev. 2002; 54:131–155.
16. Pardeike J, Hommoss A, Müller RH. Lipid nanoparticles (SLN, NLC) in cosmetic and pharmaceutical dermal products. Int J Pharm. 2009; 366(1–2):170–184. [PubMed: 18992314]
17. Patel LN, Zaro JL, Shen WC. Cell penetrating peptides: intracellular pathways and pharmaceutical perspectives. Pharm Res. 2007; 24(11):1977–1992. [PubMed: 17443399]
18. Astriab-Fisher A, Sergueev D, Fisher M, Shaw BR, Juliano RL. Conjugates of antisense oligonulceosides with the Tat and antenapedia cell-penetrating peptides: effects on cellular uptake, binding to target sequences, and biologic actions. Pharm Res. 2002; 19:744–754. [PubMed: 12134943]
19. Lo SL, Wang S. An endosomolytic Tat peptide produced by incorporation of histidine and cysteine residues as a nonviral vector for DNA transfection. Biomaterials. 2008; 29(15):2408–2414. [PubMed: 18295328]
20. Rudolph C, Schillinger U, Ortiz A, Tabatt K, Plank C, Muller RH, Rosenecker J. Application of novel solid lipid nanoparticle (SLN)-gene vector formulations based on a dimeric HIV-1 TAT-peptide in vitro and in vivo. Pharm Res. 2004; 21(9):1662–1669. [PubMed: 15497694]
21. Torchilin VP, Levechenko TS. TAT-liposomes: a novel intracellular drug carrier. Curr Prot Pept Sci. 2003; 4:133–140.
22. Lopes LB, Brophy CM, Furnish E, Flynn CR, Sparks O, Komalavilas P, Joshi L, Panitch A, Bentley MV. Comparative Study of the Skin Penetration of Protein Transduction Domains and a Conjugated Peptide. Pharm Res. 2005; 22(5):750–757. [PubMed: 15906170]
23. Patlolla RR, Vobalaboina V. Pharmacokinetics and tissue distribution of etoposide delivered in parenteral emulsion. J Pharm Sci. 2005; 94:437–445. [PubMed: 15614812]
24. Herringson TP, Patlolla RR, Altin JG. Targeting of plasmid DNA-lipoplexes to cells with molecules anchored via a metal chelator lipid. J Gene Med. 2009; 11(11):1048–1063. [PubMed: 19757485]
25. Babu RJ, Kikwai L, Jaiani LT. Percutaneous absorption and anti-inflammatory effect of a substance P receptor antagonist: Spantide II. Pharm Res. 2004; 21:108–113. [PubMed: 14984264]
26. Joshi M, Patravale V. Nanostructured lipid carrier (NLC) based gel of celecoxib. Int J Pharm. 2008; 346(1–2):124–132. [PubMed: 17651933]
27. Zhang L, Qian Y, Long C, Chen Y. Systematic Procedures for Formulation Design of Drug-Loaded Solid Lipid Microparticles: Selection of Carrier Material and Stabilizer. Ind Eng Chem Res. 2004; 47:6091–6100.
28. Wu X, Price GJ, Guy RH. Disposition of nanoparticles and an associated lipophilic permeant following topical application to the skin. Mol Pharm. 2009; 6(5):1441–1448. [PubMed: 19630400]

NIH-PA Author Manuscript

NIH-PA Author Manuscript

NIH-PA Author Manuscript

29. Chikh GG, Li WM, Schutze-Redelmeier MP, Meunier JC, Bally MB. Attaching histidine-tagged peptides and proteins to lipid-based carriers through use of metal-ion-chelating lipids. Biochim Biophys Acta. 2002; 1567(1–2):204–212. [PubMed: 12488054]
30. Puglia C, Blasi P, Rizza L, Schoubben A, Bonina F, Rossi C, Ricci M. Lipid nanoparticles for prolonged topical delivery: an in vitro and in vivo investigation. Int J Pharm. 2008; 357:295–304. [PubMed: 18343059]
31. Jung S, Otberg N, Thiede G, Richter H, Sterry W, Panzner S, Lademann J. Innovative liposomes as a transfollicular drug delivery system: penetration into porcine hair follicles. J Invest Dermatol. 2006; 126(8):1728–1732. [PubMed: 16645589]
32. Song YK, Kim CK. Topical delivery of low-molecular-weight heparin with surface-charged flexible liposomes. Biomaterials. 2006; 27(2):271–280. [PubMed: 16039711]
33. Wang X, Xu W, Mohapatra S, Kong X, Li X, Lockey RF, Mohapatra SS. Prevention of airway inflammation with topical cream containing imiquimod and small interfering RNA for natriuretic peptide receptor. Genet Vaccines Ther. 2008; 15:6–7.
34. Rothbard JB, Garlington S, Lin Q, Kirschberg T, Kreider E, Mcgrane PL, Wender PA, Khavari PA. Conjugation of arginine oligomers to cyclosporine A facilitates topical delivery and inhibition of inflammation. Nat med. 2000; 6:1253–1257. [PubMed: 11062537]
35. Vogt A, Combadiere B, Hadam S, Stieler KM, Lademann J, Schaefer H, Autran B, Sterry W, Blume-Peytavi U. 40 nm, but not 750 or 1,500 nm, nanoparticles enter epidermal CD1a+ cells after transcutaneous application on human skin. J Invest Dermatol. 2006; 126(6):1316–1322. [PubMed: 16614727]
36. Alvarez-Román R, Naik A, Kalia YN, Guy RH, Fessi H. Skin penetration and distribution of polymeric nanoparticles. J Control Release. 2004; 99(1):53–62. [PubMed: 15342180]
37. Tréhin R, Krauss U, Beck-Sickinger AG, Merkle HP, Nielsen HM. Cellular uptake but low permeation of human calcitonin-derived cell penetrating peptides and Tat(47–57) through well-differentiated epithelial models. Pharm Res. 2004; 21(7):1248–1256. [PubMed: 15290867]
38. Mélot M, Pudney PD, Williamson AM, Caspers PJ, Van Der Pol A, Puppels GJ. Studying the effectiveness of penetration enhancers to deliver retinol through the stratum cornum by in vivo confocal Raman spectroscopy. J Control Release. 2009; 138(1):32–39. [PubMed: 19401210]
39. Herkenne C, Alberti I, Naik A, Kalia YN, Mathy FX, Préat V, Guy RH. In vivo methods for the assessment of topical drug bioavailability. Pharm Res. 2008; 25(1):87–103. [PubMed: 17985216]
40. Caspers PJ, Lucassen GW, Puppels GJ. Combined in vivo confocal Raman spectroscopy and confocal microscopy of human skin. Biophys J. 2003; 85(1):572–580. [PubMed: 12829511]
41. Teeranachaideekul V, Boonme P, Souto EB, Müller RH, Junyaprasert VB. Influence of oil content on physicochemical properties and skin distribution of Nile red-loaded NLC. J Control Release. 2008; 128(2):134–141. [PubMed: 18423768]

NIH-PA Author Manuscript
NIH-PA Author Manuscript
NIH-PA Author Manuscript

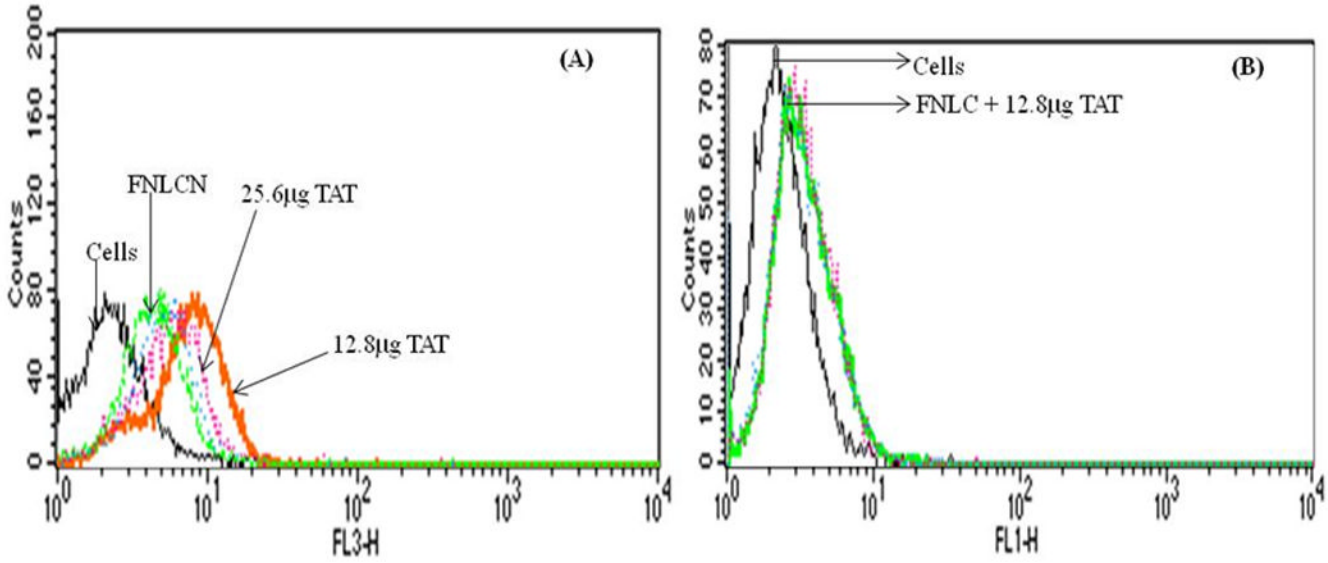

Figure 1.

Binding assay of NLC nanoparticles with and without TAT peptide in H460 cell lines. The amount of TAT peptide was optimized with respect to DOGS-NTA-Ni concentration. A) Binding of FNLCN with various amounts of TAT peptide. Increase in TAT peptide concentration above 12.8 µg to 25.6 µg decreased the binding (line is not clear because mixed with blue line of 6.4 µg). B) FNLC formulations without DOGS-NTA-Ni prepared with Dio-dye, incubated with 12.8 µg TAT peptide showed very small non-specific binding.

NIH-PA Author Manuscript

NIH-PA Author Manuscript

NIH-PA Author Manuscript

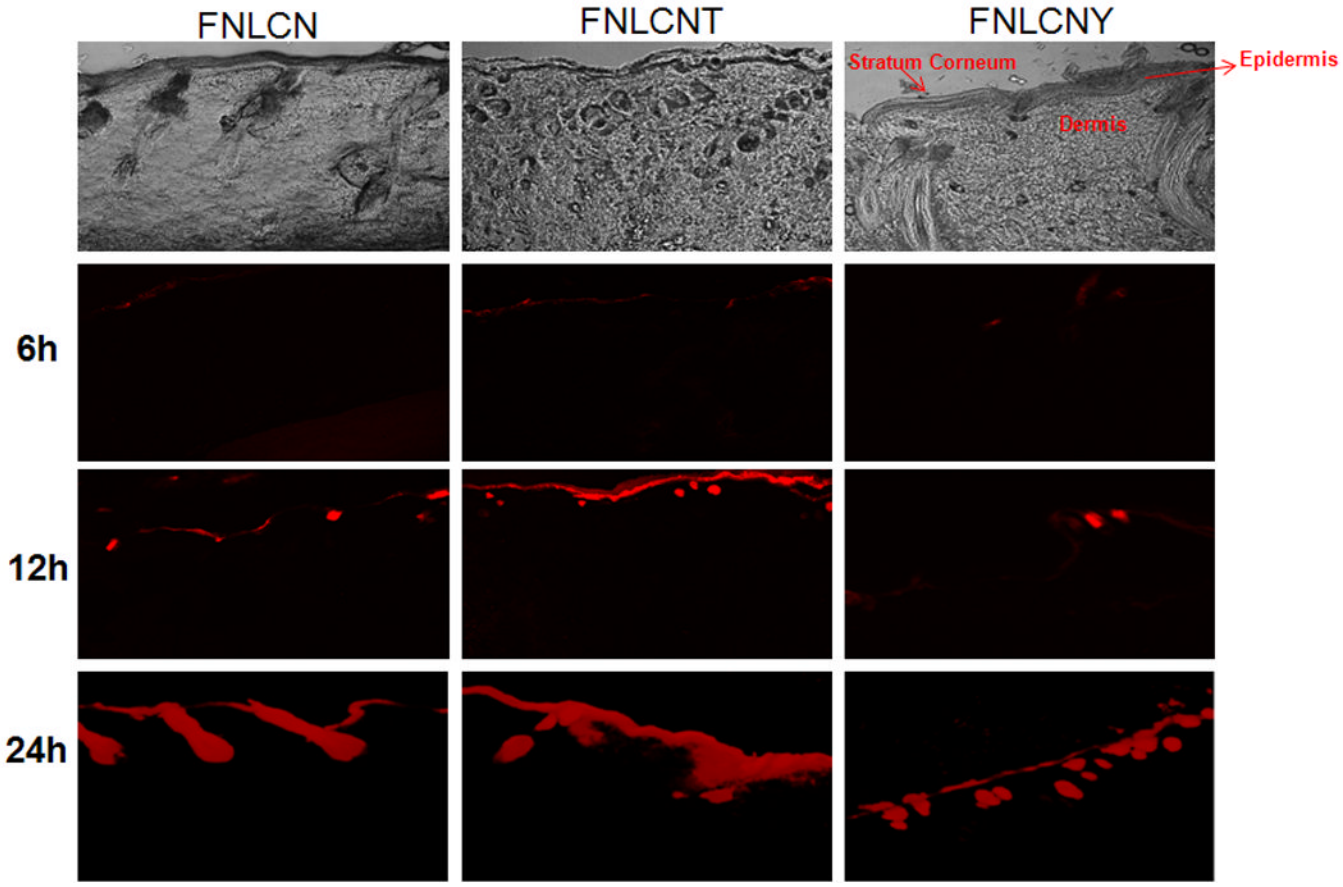

Figure 2.

In-vitro rat skin permeation of lipophilic DID fluorescent dye encapsulated with and without CPP coated NLCN nanoparticles, the vertical skin sections with a thickness of 30 μm thick were made with cryotome and observed under confocal microscope for skin associated fluorescence. As a control NLC formulation without DOGS-NTA was encapsulated with DID-dye, the permeation studies lasted for 24 h and all the confocal images were taken using 10× objective. The bottom row shows the overlay of bright field and fluorescence. Results indicate that surface modification of nanoparticles with CPP enhanced the skin permeation, whereas addition of non-transduction peptide (YKA) inhibited the entry of nanoparticles into the skin.

NIH-PA Author Manuscript
NIH-PA Author Manuscript
NIH-PA Author Manuscript

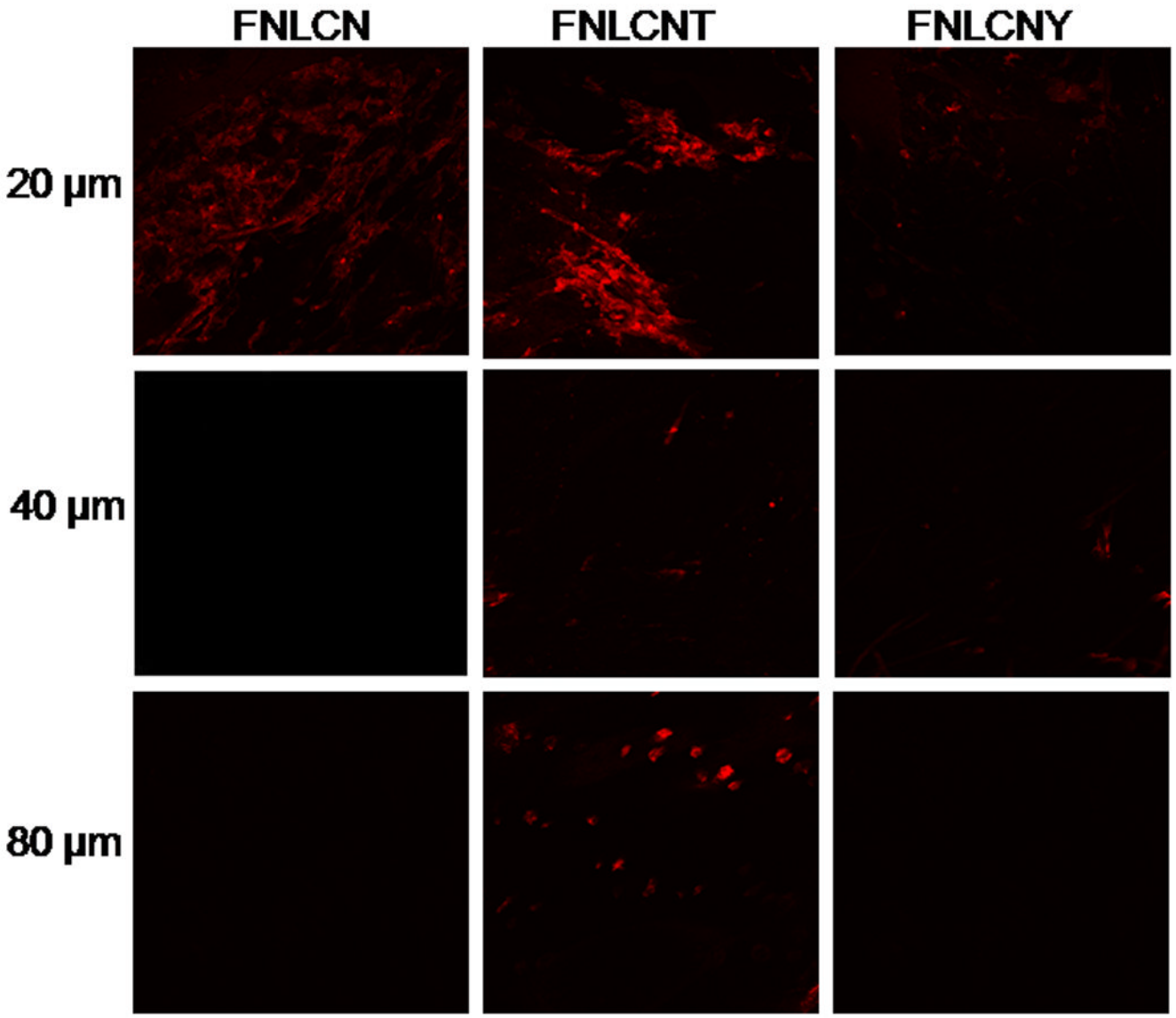

Figure 3.

In-vitro rat skin permeation of lipophilic DID fluorescent dye encapsulated with and without CPP coated NLCN nanoparticles, after 6 h of skin permeation of FNLCN, FNLCNT and FNLCNY formulations the lateral skin sections were made to a depth of 160 μm with cryotome and observed under confocal microscope for skin associated fluorescence. In this figure, the 120 and 160 μm depths skin section figures were not presented because at below 80 μm skin depths we didn't observe any skin associated fluorescence with all formulations. Vertical row indicate the depth of skin sections.

NIH-PA Author Manuscript

NIH-PA Author Manuscript

NIH-PA Author Manuscript

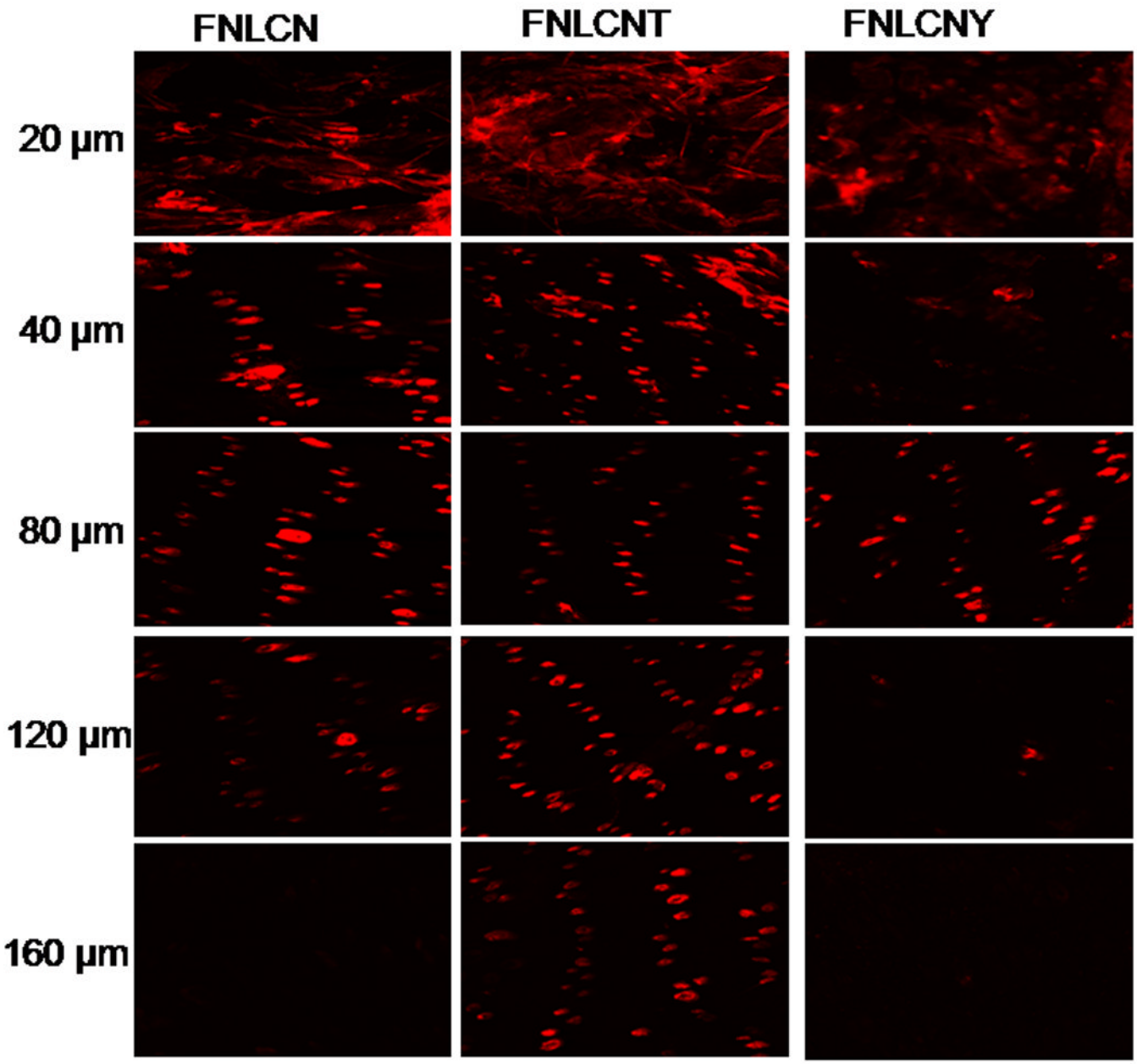

Figure 4.

In-vitro rat skin permeation of lipophilic DID fluorescent dye encapsulated with and without CPP coated NLCN nanoparticles, after 12 h of skin permeation of FNLCN, FNLCNT and FNLCNY formulations the lateral skin sections were made to a depth of 160 µm with cryotome and observed under confocal microscope for skin associated fluorescence. Vertical row show the depth of skin sections.

NIH-PA Author Manuscript

NIH-PA Author Manuscript

NIH-PA Author Manuscript

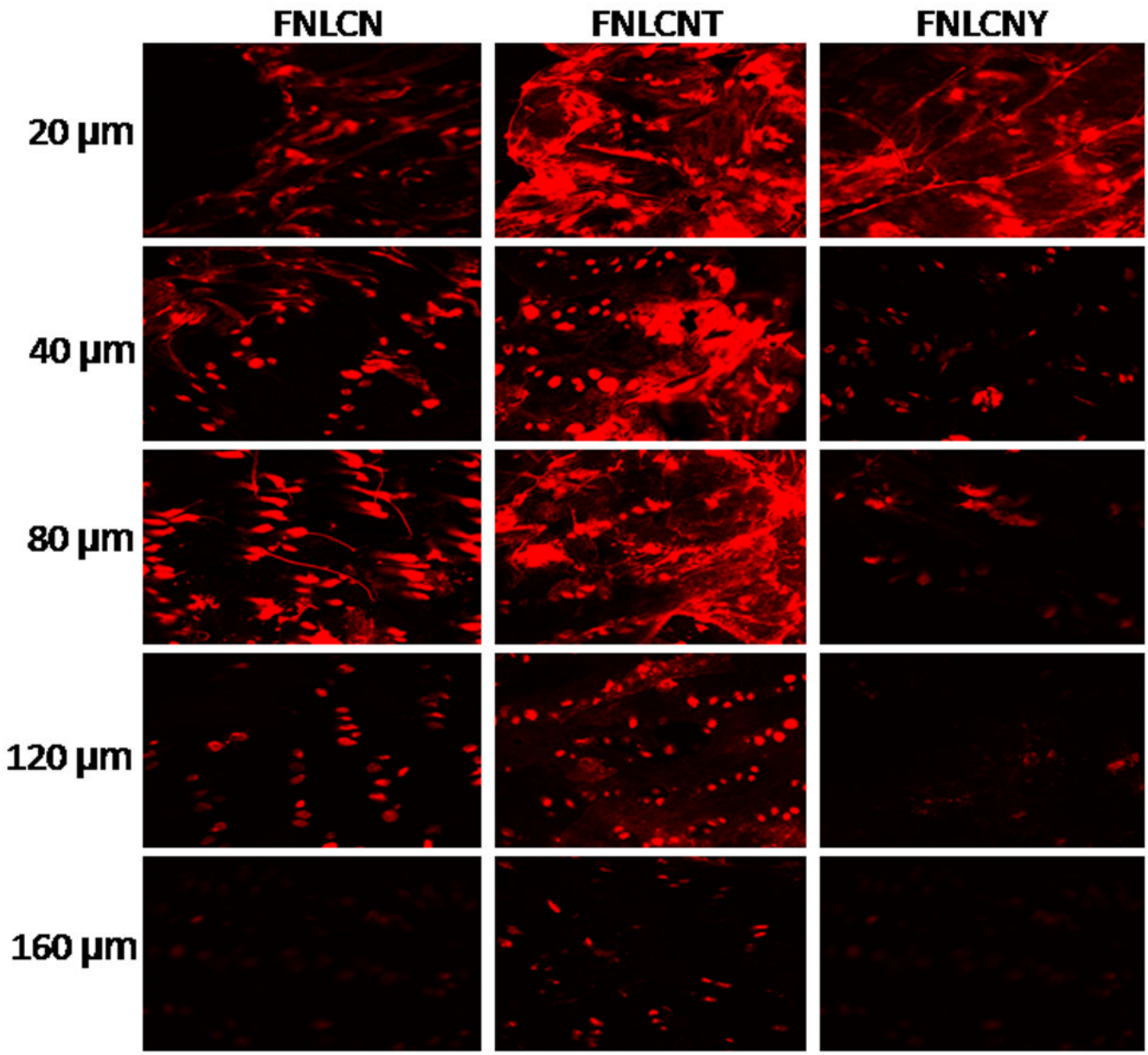

Figure 5.

In-vitro rat skin permeation of lipophilic DID fluorescent dye encapsulated with and without CPP coated NLCN nanoparticles, after 24 h of skin permeation of FNLCN, FNLCNT and FNLCNY formulations the lateral skin sections were made to a depth of 160 µm with cryotome and observed under confocal microscope for skin associated fluorescence. Vertical row indicate the depth of the skin sections.

NIH-PA Author Manuscript
NIH-PA Author Manuscript
NIH-PA Author Manuscript

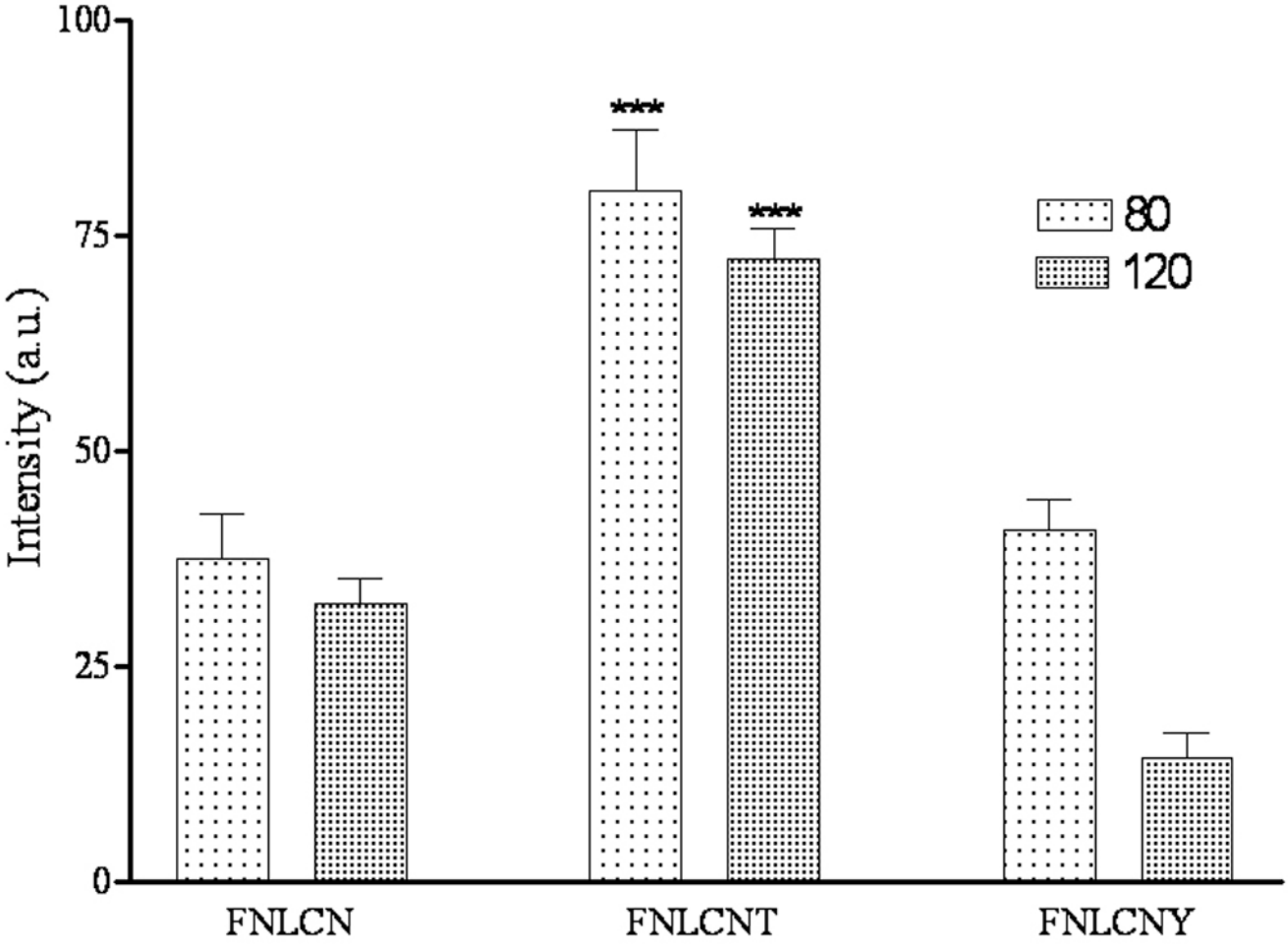

Figure 6.

Shift in the fluorescence intensity of lateral skin sections after 24 h of skin permeation with FNLCN, FNLCNT and FNLCNY formulations observed under confocal Raman spectroscope. Data represent mean ± SEM, n=3; significance FNLCNT against FNLCN and FNLCNY, ***$p < 0.001$.

NIH-PA Author Manuscript

NIH-PA Author Manuscript

NIH-PA Author Manuscript

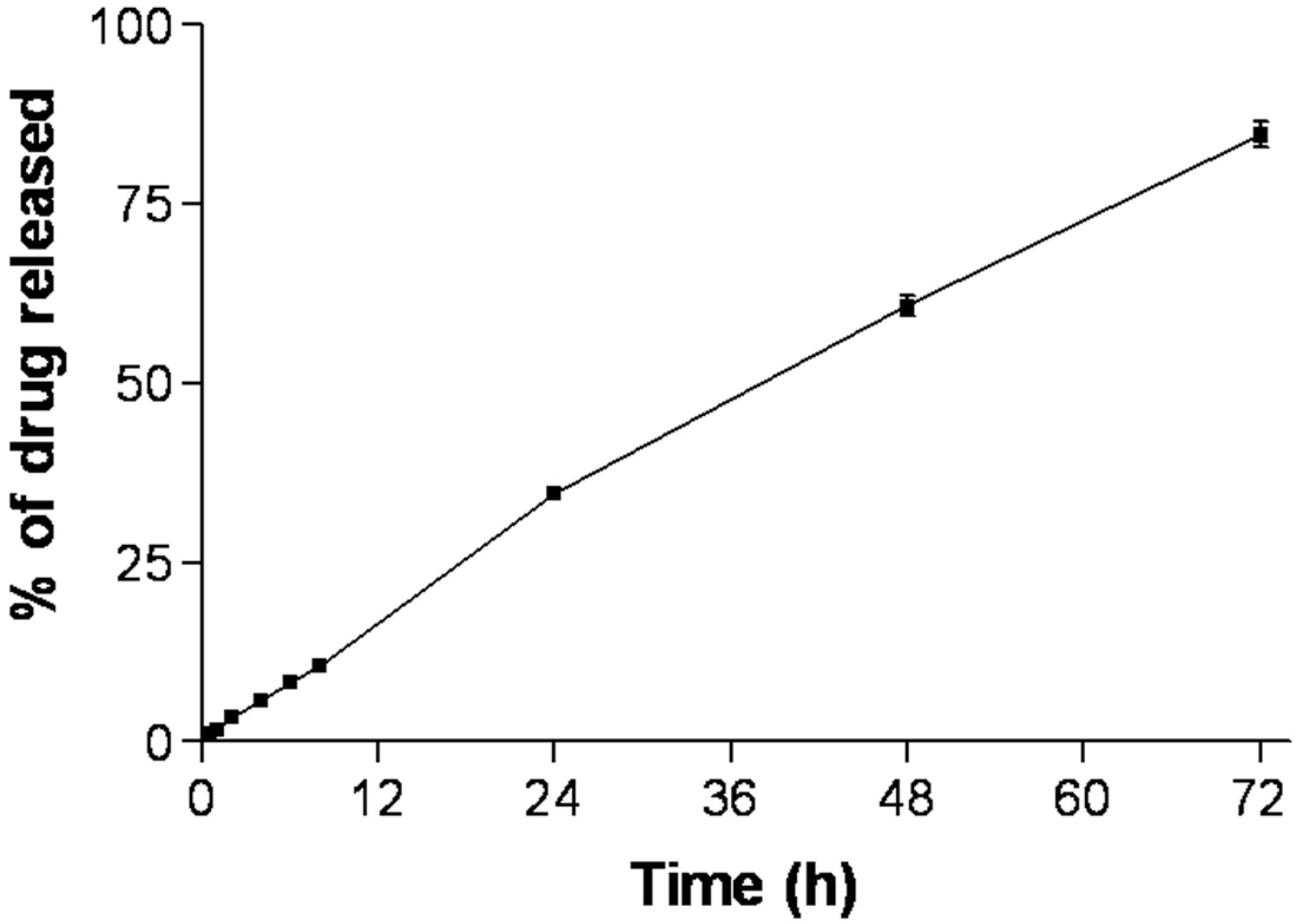

Figure 7.
In-vitro release of Cxb encapsulated NLCN formulation.

NIH-PA Author Manuscript

NIH-PA Author Manuscript

NIH-PA Author Manuscript

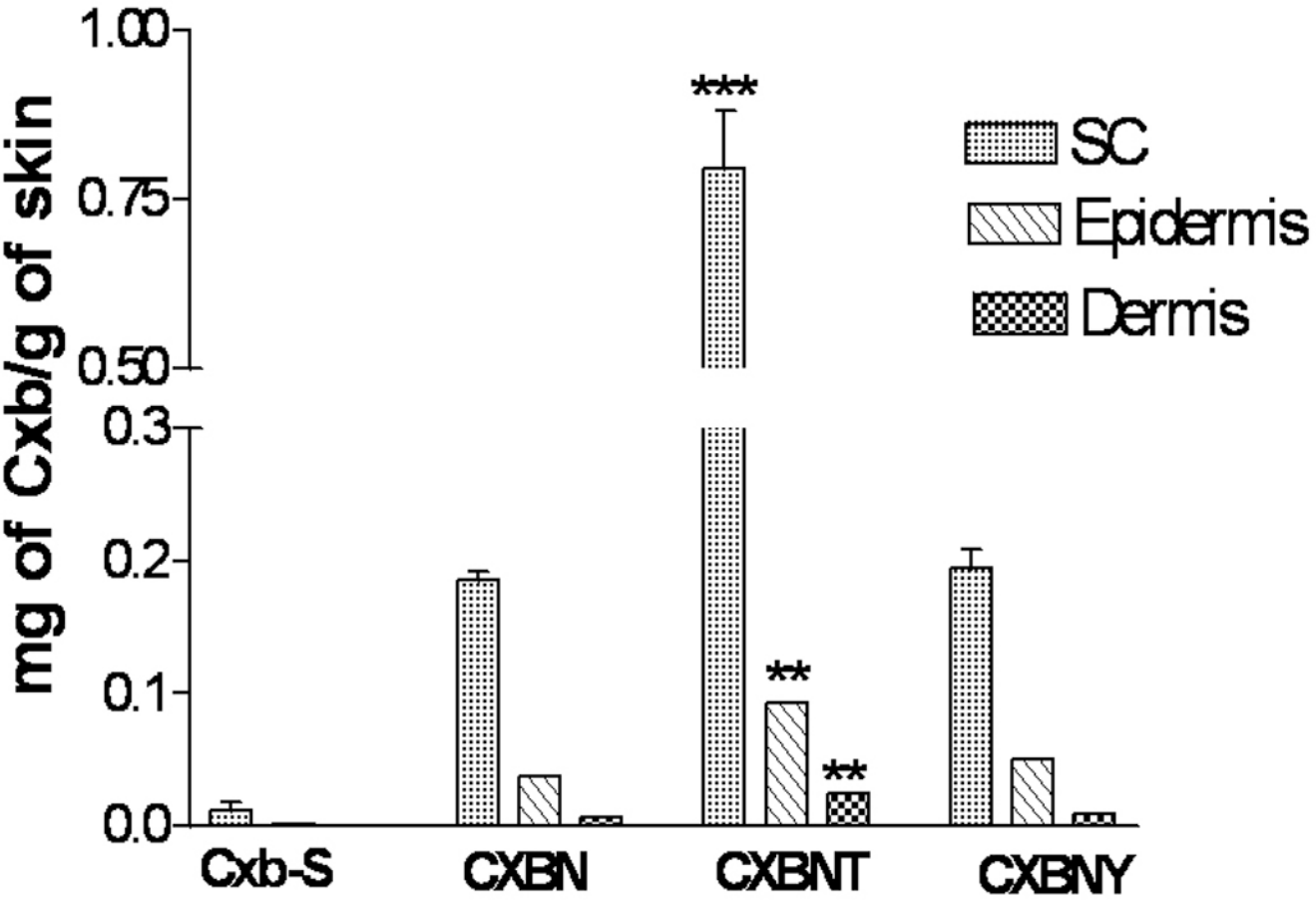

Figure 8.

Effect of TAT peptide on the skin permeation of Cxb encapsulated NLCN formulations. In vitro skin permeation studies were carried out in full thickness rat skin using Franz diffusion cells and after 24 h of application, the skin was collected and processed as described in methods section. Data represent mean ± SEM, n=4, significance FNLCNT against FNLCN and FNLCNY where *** $p < 0.001$ ** $p < 0.05$.